INTERNATIONAL JOURNAL FOR NUMERICAL METHODS IN FLUIDS
Int. J. Numer. Meth. Fluids 2009; **61**:119–143
Published online 5 November 2008 in Wiley InterScience (www.interscience.wiley.com). DOI: 10.1002/fld.1940

A model for the dynamics of rowing boats

Luca Formaggia*,†, Edie Miglio, Andrea Mola and Antonio Montano

MOX, Dipartimento di Matematica, Politecnico di Milano, Via Bonardi 9, Milano, Italy

SUMMARY

A model of a rowing scull has been developed, comprising the full motion in the symmetry plane and the interaction with the hydrodynamics. A particular emphasis has been given to the energy dissipation due to the secondary movements activated by the motion of the rowers and the intermittent forcing terms. Numerical simulations show the effectiveness of the proposed procedure. Copyright © 2008 John Wiley & Sons, Ltd.

Received 13 April 2008; Revised 30 August 2008; Accepted 2 September 2008

KEY WORDS: computational fluid dynamics; sport engineering; dynamical systems

1. INTRODUCTION

This work concerns the numerical modeling of the dynamics of extremely narrow and light rowing boats specifically designed for competition or exercise. These racing shells are designed to have a low drag, to increase speed even if at the price of a relatively low stability.

Indeed, rowing is a sport with a long-standing tradition and the search for performance has selected the best athletic gestures, as well as the shape and materials for all boat's elements. Nowadays, further significant enhancements can be obtained through mathematical models and computer simulations, possibly integrated with CAD/CAM systems. This work is an attempt to provide a computationally efficient, yet rather complete, numerical model for the full dynamics of rowing sculls.

Two are the most common types of rowing boats, which reflect the two major techniques of rowing: sweeping and sculling. In sweep boats each rower has one oar, and holds it with both hands. Rowers holding the left and right oar sit on the boat in an alternate fashion. In a scull instead, each rower uses two oars (left and right), and move them synchronously. In both cases, the rowers sit with their back to the direction the boat is moving and power is generated using a

*Correspondence to: Luca Formaggia, MOX, Dipartimento di Matematica, Politecnico di Milano, Via Bonardi 9, Milano, Italy.
†E-mail: luca.formaggia@polimi.it

blended sequence of the action of legs, back and arms. Each rower sits on a sliding seat wheeling on a track called the slide. Sometimes a coxswain is added to the crew, who is a person who steers the shell using a small rudder and urges the rowers on giving the rhythm to their movements.

The modeling of the dynamics of a rowing scull is made difficult by the strong unsteadiness of the rowers motion and the interaction of the boat with the free surface. While studies of the steady-state flow around boats moving at constant speed are nowadays rather well-established design tools, they provide only partial information on the sculls hydrodynamic efficiency. Indeed, the varying forces at the oars and most importantly the inertial forces due to the movement of the rowers, superimpose to the mean motion a complex system of secondary movements, which in a first approximation, may be considered periodic. These secondary movements induce an additional drag mainly because of the generated gravity wave, which radiates away from the boat dissipating energy. Their account in the design process could improve the overall performance of the scull. Furthermore, a simulator incorporating the rowers motion with a sufficient detail could also be used by trainers to understand the effects of different rowing styles or crew composition.

Since the early works of Alexander [1], the topic of rowing boats dynamics in sculls has been widely investigated, although most of the technical reports produced have been published only on the world wide web. Some of the most interesting contributions are those by Atkinson [2], Dudhia [3] and van Holst [4]. In [5] Lazauskas provides a rather complete mathematical model for boat dynamics. However, all these models focus only on horizontal movements and use empirical formulas to simulate dissipative effects. The contribution of the vertical movement (heaving) and angular rotation (pitching) of the boat is indeed neglected.

Moreover, a few essays on stroke dynamics have been published in the context of the design of rowing machines. We cite the works of Elliott and others [6], and that of Rekers [7]. Their aim is rather different from ours, namely to try to reproduce a realistic rowing movement in the machine. Again, only the horizontal motion has been considered, being the only reproducible by current rowing machines.

In this work, we consider instead the full movement of the scull in the symmetry plane, including horizontal motion, pitching and heaving. The assumption that the motion lies in the boat symmetry plane is reasonable for sculls, and greatly simplifies the calculations. We here recall that in a scull each rower holds two oars, and experienced scullers are able to move them synchronously and with great precision to keep the forward motion straight. On the contrary, the yawing movement could become relevant in the case of a sweep rowing boat, where each rower acts on a single oar and the longitudinal symmetry is easily broken.

The dynamic model is defined mainly through the boat geometry, the rowers movement, the forces at the oars and the hydrodynamic forces. Here, for the sake of efficiency, we have chosen to simulate the effect of shape, wave and viscous drag by standard formulas, while hydrostatic forces, which depend on the wetted surface, are dynamically computed. The dissipative effects of waves generated by the secondary movements are dealt with by using a linear approximation of the water dynamics and the fluid–structure interaction. It turns out that they are equivalent to adding mass and damping terms to the dynamic model. The rowers motion relative to the boat has been obtained from motion capture measurements, while the description of the forces at the oars have been taken from literature data. Finally, the coefficients for the viscous and wave drag have been estimated by performing a few 'off-line' stationary Reynolds Averaged Navier–Stokes (RANS) computations on the actual scull geometry.

The technique here proposed contains several approximations compared with a full dynamic RANS model like the one used, for instance, in [8, 9]. Yet, it is able to provide reasonable answers

DOI: 10.1002/fld

in a matter of minutes instead of several hours. For this reason, it is currently adopted to aid the preliminary design process of racing sculls.

We point out that the assumption made on the symmetry of the motion is not fundamental, most of the equations derived in this work are readily extended to the general case.

The organization of the paper is as follows. The next section gives an overview of the dynamical model. Section 3 deals with the choice of the reference systems used to describe the motion. In Section 4 we deal with the system of equations describing boat dynamics and in Section 5 we explain how we have modeled the rowers motion and forces. The fluid–structure interaction model is given in Section 6. Finally, in Section 7 we present a few numerical results obtained using the proposed model.

2. MODEL DESCRIPTION

Before going any further in the formulation of the model, it may be useful to describe briefly the main components of a rowing boat, and introduce some terminology (see Figure 1).

In the kind of boats at hand, rowers sit in the central part of an elongated hull with their back pointing toward the advancing direction of the boat. The seats slide on rails, whereas the rowers feet are secured to foot stretchers (or footboards), usually by means of a pair of sneakers permanently attached to each footboard. The oars are linked to the hull by means of oarlocks mounted on lateral supports named outriggers (or just riggers). In our model, oarlocks are represented as perfect spherical joints. There are different types of sculls, single (1x), double (2x), quad (4x) and eight (8x). They can be coxswained or coxswainless. In our model the possible presence of a coxswain may be considered by adding an additional fixed mass. For the sake of simplicity, we have reported

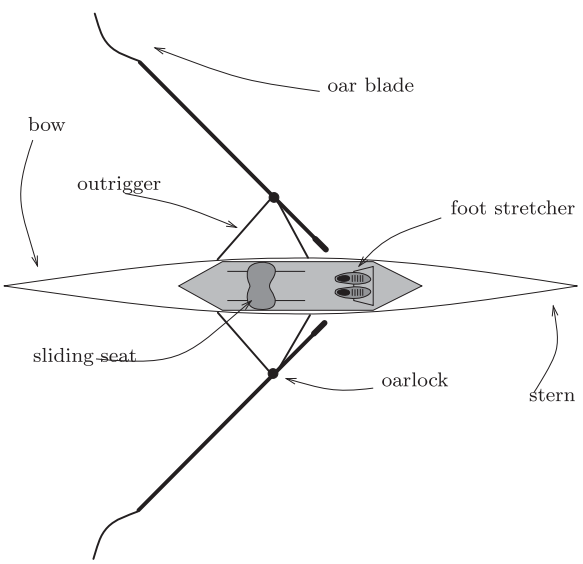

Figure 1. A single scull with the main components.

DOI: 10.1002/fld

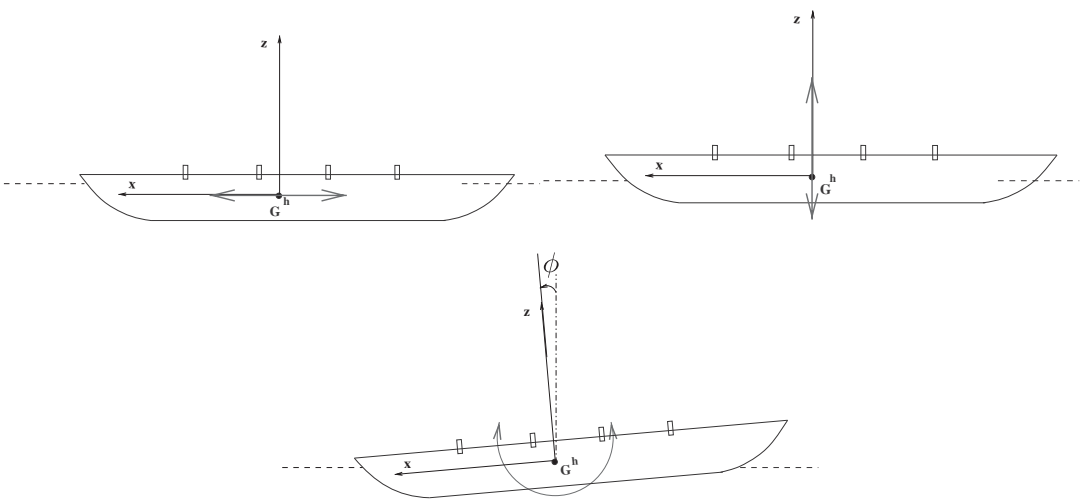

Figure 2. Secondary movements produced by rowers action. From left to right: horizontal acceleration, sinking and pitching.

in this paper the derivation for a coxswainless scull, the modification for a coxswained boat being straightforward.

The instantaneous velocity of a point of the boat can be split into two components. A mean velocity $\bar{\mathbf{V}}$ and secondary motions $\mathbf{u}$. That is

$$\mathbf{V}(\mathbf{X},t)=\bar{\mathbf{V}}(\mathbf{X},t)+\mathbf{u}(\mathbf{X},t)$$

at any point of the boat and for all $t>0$ (we take $t=0$ the starting time). The secondary motions are those induced by the rowers movement and by the action of the oars, and they are assumed periodic with period equal to the cadence of the rowing action. We also assume that the mean motion is linear and that its time scale is greater than that of the secondary motion. Indeed, if we neglect the starting phase, we can assume that $\bar{\mathbf{V}}$ is practically constant.

We will consider the motion in the symmetry plane of the boat and Figure 2 shows the three secondary motions. The first is an horizontal linear motion along the boat longitudinal axis. It is originated mainly by the intermittent traction and the horizontal displacement of the rowers. We will refer to it as the *horizontal* secondary motion. A second motion is along the vertical axis, and can be though as a fluctuation around the hydrodynamic equilibrium position. We will denote it as *sinking* motion. It is generated by the rowers mainly during the so-called *drive* phase of the stroke, when they push against the foot stretchers and pull on the oars to force the blade through the water. This action produces a force with a vertical component. Finally, the rowers center of mass moves because of the rotation of the shoulders and the seat sliding back and forth inside the boat. The combination of these effects leads to a change in the angular inertia of the boat that is counterbalanced by a rotational motion, which we indicate by *pitching*.

To carry out the analysis we have considered three different interacting subsystems. Namely:

1. The *hull*. It is assumed to be a rigid body of known mass and angular inertia since the sliding seats have a negligible mass. Its center of mass will be indicated by $\mathbf{G}^{\mathrm{h}}$ and its position is one of the unknowns of our mathematical model.

DOI: 10.1002/fld

2. The *rowers*. In most cases their mass is largely prevailing that of the hull. We assume that each rower can be approximated by a set of point masses corresponding to the main body parts and moving in accordance to a model of rowers motion.
3. The *oars*. Oars are assumed to act as perfect levers with negligible mass and to have 'perfect blades'. Thus, the lever fulcrum is positioned at the oar blade. This latter hypothesis can be weakened by using a more detailed model of the blade action.

3. REFERENCE SYSTEMS

Any attempt to model the dynamics of a rowing boat should start from an accurate geometrical description of the boat. More precisely, the values for footboards, seats and oarlocks positions, oars lengths, etc. must be provided, as well as the geometry of the external surface. These elements are more easily given with respect to a reference system fixed on the boat, while the boat movement is conveniently described in an inertial frame of reference fixed on the race field.

Figure 3 shows a scull with two different reference frames. The inertial reference system $(\mathbf{O}; X, Y, Z)$ is fixed with the race field and we denote with $\mathbf{e}_X$, $\mathbf{e}_Y$ and $\mathbf{e}_Z$ the corresponding unit vectors. We refer to it as the *absolute* reference. The X-axis is horizontal, parallel to the undisturbed water free surface, and oriented along the direction of progression of the boat. The Z-axis is vertical and pointing upwards, while $\mathbf{e}_Y = \mathbf{e}_Z \times \mathbf{e}_X$. By convention, the origin $\mathbf{O}$ is at the start and the undisturbed water free surface is placed at the constant value $Z = h^0$.

A second reference system is moving on the boat and will be referred to as the *hull coordinate system*, $(\mathbf{G}^{\mathrm{h}}; x, y, z)$, see Figure 3. The axes, whose unit vectors are $\mathbf{e}_x$, $\mathbf{e}_y$ and $\mathbf{e}_z$, respectively, are defined so that $\mathbf{e}_x$ and $\mathbf{e}_z$ identify the hull symmetry plane and $\mathbf{e}_z$ is directed from bottom to top, whereas $\mathbf{e}_x$ is from stern to bow. We point out that the hull reference system is centered in the hull center of mass $\mathbf{G}^{\mathrm{h}}$ and not in the center of mass arising from hull and rowers system composition, the latter being not fixed due to the rowers motion.

The *pitch angle* ϕ is the angle between unit vectors $\mathbf{e}_X$ and $\mathbf{e}_x$, and is the other unknown of our problem. Angles are measured counterclockwise, hence a positive ϕ corresponds to a downwards movement of the bow.

Points in the absolute reference system will be indicated with uppercase letter, while the corresponding lowercase letter will indicate points in the hull reference frame. Vector quantities will be expressed in bold font (e.g. **f**) as for points of the Euclidean space, normal fonts will be used for scalars.

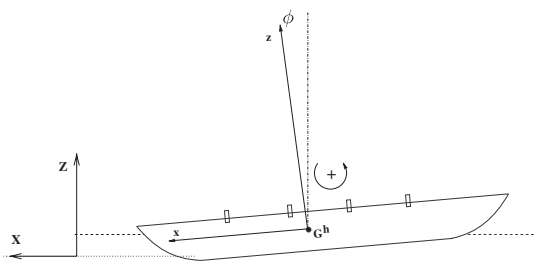

Figure 3. Rowing boat with relevant reference frames. The hull reference system is centered at hull center of mass.

DOI: 10.1002/fld

As for the components of a vector, we will use the suffices X, Y and Z to indicate their components in the absolute coordinate system, whereas x, y and z refer to the hull coordinate system. That is

$$\mathbf{f}=f_X\mathbf{e}_X+f_Y\mathbf{e}_Y+f_Z\mathbf{e}_Z$$

in the absolute coordinate system, whereas

$$\mathbf{f}=f_x\mathbf{e}_x+f_y\mathbf{e}_y+f_z\mathbf{e}_z \tag{1}$$

in the hull system. We denote with $\mathscr{R}(\phi)$ and $\mathscr{R}^{\mathrm{T}}(\phi)$ the rotation matrix and its transpose defined as

$$\mathscr{R}(\phi)=\begin{bmatrix}\cos\phi & 0 & -\sin\phi\\ 0 & 1 & 0\\ \sin\phi & 0 & \cos\phi\end{bmatrix} \quad \text{and} \quad \mathscr{R}^{\mathrm{T}}(\phi)=\begin{bmatrix}\cos\phi & 0 & \sin\phi\\ 0 & 1 & 0\\ -\sin\phi & 0 & \cos\phi\end{bmatrix} \tag{2}$$

we have

$$\begin{bmatrix}f_x\\ f_y\\ f_z\end{bmatrix}=\mathscr{R}(\phi)\begin{bmatrix}f_X\\ f_Y\\ f_Z\end{bmatrix} \quad \text{and} \quad \begin{bmatrix}f_X\\ f_Y\\ f_Z\end{bmatrix}=\mathscr{R}^{\mathrm{T}}(\phi)\begin{bmatrix}f_x\\ f_y\\ f_z\end{bmatrix} \tag{3}$$

For vectors associated to the motion (velocities, acceleration, etc.), we will also use the convention of adopting upper case letter for quantities in the absolute (inertial) frame and lower case letters for quantities related to the (non-inertial) hull reference.

Given a time-dependent vector function, $\mathbf{P}=\mathbf{P}(t)$, we will make use of the following notation:

$$\dot{\mathbf{P}}=\frac{\mathrm{d}\mathbf{P}}{\mathrm{d}t}, \quad \ddot{\mathbf{P}}=\frac{\mathrm{d}^2\mathbf{P}}{\mathrm{d}t^2}$$

Finally, with n we indicate the number of rowers.

3.1. Change of reference system

We can relate a point $\mathbf{P}=(P_X, P_Y, P_Z)$ in the absolute coordinate system and the corresponding point $\mathbf{p}=(P_x, P_y, P_z)$ in the hull coordinate system, by means of the equation

$$\mathbf{p}=\mathscr{R}(\phi)(\mathbf{P}-\mathbf{G}^{\mathrm{h}}) \tag{4}$$

The inverse transformation reads

$$\mathbf{P}=\mathscr{R}^{\mathrm{T}}(\phi)\mathbf{p}+\mathbf{G}^{\mathrm{h}} \tag{5}$$

The absolute velocity $\mathbf{V}=\dot{\mathbf{P}}$ of a generic point $\mathbf{P}$ and that relative to the hull system, $\mathbf{v}$, are related by

$$\mathbf{V}=\mathbf{v}+\dot{\mathbf{G}}^{\mathrm{h}}+\dot{\mathscr{R}}^{\mathrm{T}}\mathscr{R}(\mathbf{P}-\mathbf{G}^{\mathrm{h}})=\mathbf{v}+\dot{\mathbf{G}}^{\mathrm{h}}+\boldsymbol{\omega}\times(\mathbf{P}-\mathbf{G}^{\mathrm{h}})$$

DOI: 10.1002/fld

where $\boldsymbol{\omega}=\dot{\phi}\,\mathbf{e}_Y$ is the angular velocity vector. We have that

$$\boldsymbol{\omega}\times(\mathbf{P}-\mathbf{G}^{\mathrm{h}})=\dot{\phi}[(P_Z-G_Z^{\mathrm{h}})\mathbf{e}_X-(P_X-G_X^{\mathrm{h}})\mathbf{e}_Z]=\dot{\phi}[p_z\mathbf{e}_x-p_x\mathbf{e}_z]$$

As for the acceleration $\mathbf{A}$ of the generic point $\mathbf{P}$, the transformation between the local and the absolute reference reads

$$\mathbf{A}=\mathbf{a}+\ddot{\mathbf{G}}^{\mathrm{h}}+\dot{\boldsymbol{\omega}}\times(\mathbf{P}-\mathbf{G}^{\mathrm{h}})+\boldsymbol{\omega}\times\boldsymbol{\omega}\times(\mathbf{P}-\mathbf{G}^{\mathrm{h}})+2\boldsymbol{\omega}\times\mathbf{v}^P \tag{6}$$

In our case,

$$\dot{\boldsymbol{\omega}}\times(\mathbf{P}-\mathbf{G}^{\mathrm{h}})=\ddot{\phi}[(P_Z-G_Z^{\mathrm{h}})\mathbf{e}_X-(P_X-G_X^{\mathrm{h}})\mathbf{e}_Z]=\ddot{\phi}[p_z\mathbf{e}_x-p_x\mathbf{e}_z] \tag{7a}$$

$$\boldsymbol{\omega}\times\boldsymbol{\omega}\times(\mathbf{P}-\mathbf{G}^{\mathrm{h}})=-\dot{\phi}^2[(P_X-G_X^{\mathrm{h}})\mathbf{e}_X+(P_Z-G_Z^{\mathrm{h}})\mathbf{e}_Z]=-\dot{\phi}^2[p_x\mathbf{e}_x+p_z\mathbf{e}_z] \tag{7b}$$

and

$$2\boldsymbol{\omega}\times\mathbf{v}^P=2\dot{\phi}(v_z\mathbf{e}_x-v_x\mathbf{e}_z) \tag{7c}$$

The previous relations may be simplified by introducing the matrix

$$\mathscr{C}(\phi)=\frac{\mathrm{d}}{\mathrm{d}\phi}\mathscr{R}(\phi)=\begin{bmatrix}-\sin\phi & 0 & -\cos\phi\\ 0 & 1 & 0\\ \cos\phi & 0 & -\sin\phi\end{bmatrix}$$

obtaining

$$\mathbf{P}=\mathbf{G}^{\mathrm{h}}+\mathscr{R}(\phi)\mathbf{p} \tag{8a}$$

$$\ddot{\mathbf{P}}=\ddot{\mathbf{G}}^{\mathrm{h}}+\mathscr{R}(\phi)\ddot{\mathbf{p}}+2\dot{\phi}\mathscr{C}(\phi)\dot{\mathbf{p}}+\ddot{\phi}\mathscr{C}(\phi)\mathbf{p}-\dot{\phi}^2\mathscr{R}(\phi)\mathbf{p} \tag{8b}$$

which link absolute and relative velocities and accelerations, respectively.

For the sake of generality, we have set the previous equations in the three-dimensional space, even if we have already assumed that the motion is planar.

4. THE EQUATIONS OF THE DYNAMICAL MODEL

We now want to write a set of equations describing the boat motion, in order to compute at each time the hull position in the absolute reference system. The latter is completely described by three degrees of freedom, as represented by the free coordinates

$$(G_X^{\mathrm{h}}, G_Z^{\mathrm{h}}, \phi) \tag{9}$$

To describe it, we will first analyze the dynamics of the three subsystems, namely hull, rowers and oars. Figure 4 is a sketch of a 4x scull where the principal positions and forces are shown.

DOI: 10.1002/fld

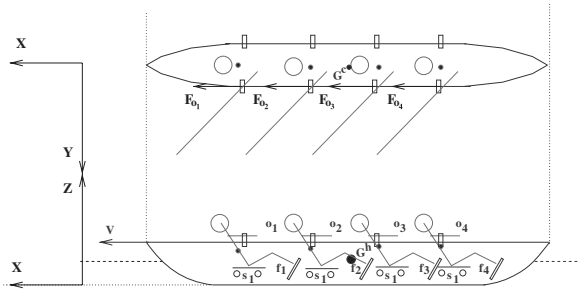

Figure 4. Quad (4x) rowing boat and absolute reference frame.

4.1. The dynamics of the hull

The dynamics of the hull may be described by the following system of equations:

$$M\ddot{\mathbf{G}}^{\mathrm{h}} = \sum_{j=1}^{n} \mathbf{F}_{\mathrm{o}_j} + \sum_{j=1}^{n} \mathbf{F}_{\mathrm{s}_j} + \sum_{j=1}^{n} \mathbf{F}_{\mathrm{f}_j} + M\mathbf{g} + \mathbf{F}^{\mathrm{w}} \tag{10a}$$

$$I_{YY}\ddot{\phi} = \sum_{j=1}^{n} (\mathbf{X}_{\mathrm{o}_j} - \mathbf{G}^{\mathrm{h}}) \times \mathbf{F}_{\mathrm{o}_j} + \sum_{j=1}^{n} (\mathbf{X}_{\mathrm{s}_j} - \mathbf{G}^{\mathrm{h}}) \times \mathbf{F}_{\mathrm{s}_j} + \sum_{j=1}^{n} (\mathbf{X}_{\mathrm{f}_j} - \mathbf{G}^{\mathrm{h}}) \times \mathbf{F}_{\mathrm{f}_j} + \mathbf{M}^{\mathrm{w}} \tag{10b}$$

where I_{YY} is the angular inertia of the hull in the Y direction and relative to the hull center of mass, $\mathbf{g}$ is the gravity acceleration and M is the mass of the hull.

On the right-hand side we have the external forces and angular momenta applied to the boat hull (see Figure 5). Those due to the interaction with the surrounding fluid are indicated with $\mathbf{F}^{\mathrm{w}}$ and $\mathbf{M}^{\mathrm{w}}$ and will be analyzed in detail in Section 6.

As for $\mathbf{F}_{\mathrm{o}_j}$, $\mathbf{F}_{\mathrm{s}_j}$, $\mathbf{F}_{\mathrm{f}_j}$, they indicate the external forces exerted by the jth rower on oarlocks, seats and footboards, respectively, They can be obtained from the equations governing the dynamics of the rowers. We remark that each $\mathbf{F}_{\mathrm{o}_j}$ and $\mathbf{F}_{\mathrm{f}_j}$ does indeed indicate the resultant of a pair of forces of equal intensity applied at each oarlock and foot, respectively.

4.2. Equations of motion for the rowers

We represent the mass distribution of an athlete of given characteristics (weight, height, sex) by subdividing the body into $p = 12$ parts of which we infer the mass m_{ij} from anatomical tables taken from [10], see Figure 6. Each part is then considered as concentrated in its own center of mass $\mathbf{X}_{ij}$, i.e. we neglect the angular inertia. The momentum equations for the jth rower is then given by the following system:

$$\sum_{i=1}^{p} m_{ij}(\ddot{\mathbf{X}}_{ij} - \mathbf{g}) = \mathbf{F}_{\mathrm{h}_j} + \mathbf{F}_{\mathrm{s}_j} + \mathbf{F}_{\mathrm{f}_j} \tag{11a}$$

$$\sum_{i=1}^{p} m_{ij}(\mathbf{X}_{ij} - \mathbf{G}^{\mathrm{h}}) \times (\ddot{\mathbf{X}}_{ij} - \mathbf{g}) = (\mathbf{X}_{\mathrm{h}_j} - \mathbf{G}^{\mathrm{h}}) \times \mathbf{F}_{\mathrm{h}_j} \times (\mathbf{X}_{\mathrm{s}_j} - \mathbf{G}^{\mathrm{h}}) \times \mathbf{F}_{\mathrm{s}_j} + (\mathbf{X}_{\mathrm{f}_j} - \mathbf{G}^{\mathrm{h}}) \times \mathbf{F}_{\mathrm{f}_j} \tag{11b}$$

DOI: 10.1002/fld

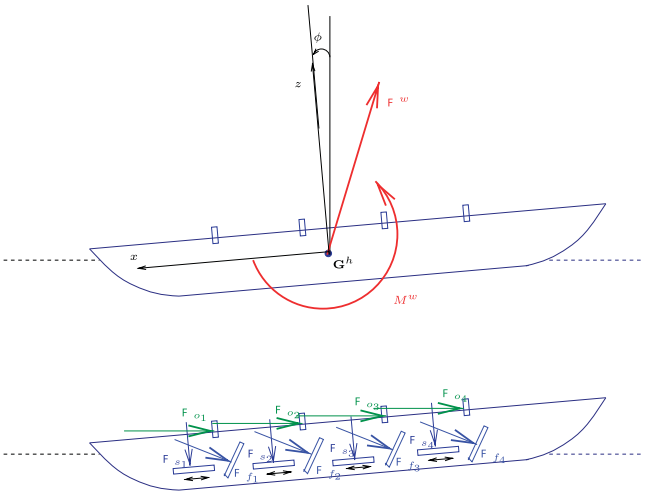

Figure 5. A sketch of the forces acting on the scull.

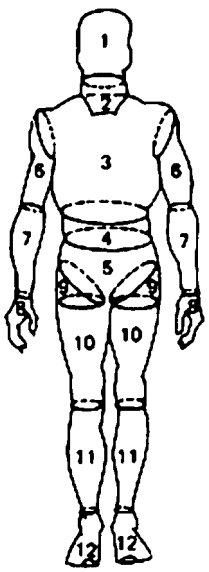

Figure 6. The 12 anatomical parts used to subdivide the body mass.

Angular momentum is computed around the hull barycenter $\mathbf{G}$. $\mathbf{F}_{\mathrm{h}_j}$ is the force at the hand of the jth athlete, while $\mathbf{X}_{\mathrm{h}_j}$, $\mathbf{X}_{\mathrm{s}_j}$ and $\mathbf{X}_{\mathrm{f}_j}$ are the positions of the hands, seats and footboards, respectively.

4.3. The dynamics of the oars

We assume that the oar is an ideal lever, having negligible mass and infinite rigidity, so that all the forces and momenta acting on it are always balanced. Under these hypotheses, the values for the

DOI: 10.1002/fld

hands and oarlocks forces $\mathbf{F}_\mathrm{h}$ and $\mathbf{F}_\mathrm{o}$ are proportional, the coefficient of proportionality depending on the geometrical configuration of the boat. The forces acting on the each oar are $-\mathbf{F}_\mathrm{o}$, $-\mathbf{F}_\mathrm{h}$, and $\mathbf{F}_\mathrm{w}$, which corresponds to the action exerted by water on the oar blade.

By the balance of force and momenta we get that (see Figure 7)

$$\mathbf{F}_\mathrm{h} = -\frac{L - r_\mathrm{h}}{L}\mathbf{F}_\mathrm{o} \tag{12}$$

Clearly, this simple model could be bettered by having a more detailed description of blade–water interaction and on the geometry of the oar movement. It has been found, however, quite sufficient for the purpose of this work.

4.4. Equations of motion for the hull–rowers system

Substituting into Equations (10) the values of $\mathbf{F}_{\mathrm{s}_i} + \mathbf{F}_{\mathrm{f}_i}$ obtained by (11a) and the values of $(\mathbf{X}_{\mathrm{s}_i} - \mathbf{G}^\mathrm{h}) \times \mathbf{F}_{\mathrm{s}_i} + (\mathbf{X}_{\mathrm{f}_i} - \mathbf{G}^\mathrm{h}) \times \mathbf{F}_{\mathrm{f}_i}$ obtained from Equation (11b) we get

$$M(\ddot{\mathbf{G}}^\mathrm{h} - \mathbf{g}) = \frac{r_\mathrm{h}}{L}\sum_{j=1}^{n}\mathbf{F}_{\mathrm{o}_j} - \sum_{j=1}^{n}\sum_{i=1}^{p} m_{ij}(\ddot{\mathbf{X}}_{ij} - \mathbf{g}) + \mathbf{F}^\mathrm{w} \tag{13a}$$

$$I_{YY}\ddot{\phi} = \sum_{j=1}^{n}\left[(\mathbf{X}_{\mathrm{o}_j} - \mathbf{G}^\mathrm{h}) - \frac{L - r_\mathrm{h}}{L}(\mathbf{X}_{\mathrm{h}_j} - \mathbf{G}^\mathrm{h})\right] \times \mathbf{F}_{\mathrm{o}_j} - \sum_{j=1}^{n}\sum_{i=1}^{p}(\mathbf{X}_{ij} - \mathbf{G}^\mathrm{h}) \times m_{ij}(\ddot{\mathbf{X}}_{ij} - \mathbf{g}) + \mathbf{M}^\mathrm{w} \tag{13b}$$

Employing Equations (8) to express rowers body parts positions and accelerations in the hull reference frame, we get the final system of ordinary differential equations for the unknowns $\mathbf{G}^\mathrm{h}$ and ϕ, where with $M^\mathrm{r} = \sum_{i,j} m_{ij}$ and $M^\mathrm{t} = M + M^\mathrm{r}$ we indicate the total mass of the rowers and

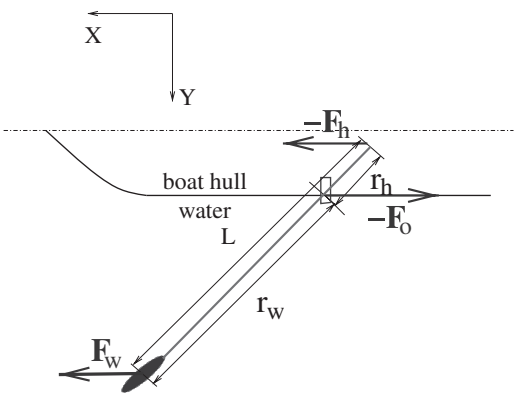

Figure 7. Oar dynamical model with all the applied forces.

DOI: 10.1002/fld

that of the scull, encompassing both rowers and hull, respectively. Namely,

$$M^{\mathrm{t}}\ddot{\mathbf{G}}^{\mathrm{h}}+\mathscr{O}(\phi)\sum_{i,j}m_{ij}\mathbf{x}_{ij}\ddot{\phi}+2\mathscr{O}(\phi)\sum_{i,j}m_{ij}\dot{\mathbf{x}}_{ij}\dot{\phi}-\mathscr{R}(\phi)\left(\sum_{i,j}m_{ij}\mathbf{x}_{ij}\right)\dot{\phi}^2$$

$$=-\mathscr{R}(\phi)\sum_{j,j}m_{ij}\ddot{\mathbf{x}}_{ij}+\frac{r_{\mathrm{h}}}{L}\sum_{j=1}^{n}\mathbf{F}_{\mathrm{o}_j}+M^{\mathrm{t}}\mathbf{g}+\mathbf{F}^{\mathrm{w}} \tag{14a}$$

and

$$\mathscr{R}(\phi)\sum_{i,j}m_{ij}\mathbf{x}_{ij}\times\ddot{\mathbf{G}}^{\mathrm{h}}+\left(I_{YY}+\sum_{i,j}m_{ij}|\mathbf{x}_{ij}|^2\right)\ddot{\phi}+2\sum_{i,j}m_{ij}\mathscr{R}(\phi)\mathbf{x}_{ij}\times\mathscr{O}(\phi)\dot{\mathbf{x}}_{ij}\dot{\phi}$$

$$=-\mathscr{R}(\phi)\sum_{i,j}m_{ij}\mathbf{x}_{ij}\times\mathscr{R}(\phi)\ddot{\mathbf{x}}_{ij}+\mathscr{R}(\phi)\sum_{i}\left(x_{\mathrm{o}_i}-x_{h_i}+\frac{r_{\mathrm{h}}}{L}x_{\mathrm{h}_i}\right)\times F_{\mathrm{o}_i}$$

$$+\mathscr{R}(\phi)\sum_{i,j}m_{ij}\mathbf{x}_{ij}\times\mathbf{g}+\mathbf{M}^{\mathrm{w}} \tag{14b}$$

where in $\sum_{i,j}$ the indexes i and j run from 1 to p and 1 to n, respectively.

To close Equations (14) we need to provide adequate models for the motion law of the rowers, oarlock forces and the fluid–dynamic forces and momenta $\mathbf{F}^{\mathrm{w}}$ and $\mathbf{M}^{\mathrm{w}}$. These will be described in next sections.

5. A MODEL FOR THE ROWERS MOTION AND FORCES

The athletes move periodically on the boat with a cadence r that in race conditions is between 30 and 40 strokes per minute. Each stroke can be divided into two phases. In the *active* phase, the oar blades are in the water, and the rowers exert on the hull both inertial and traction forces. In the *recovery* phase, the athletes extract the oar blades from the water and return to the initial position, to get ready for another stroke. In this phase the athletes exert on the hull only inertial forces.

The ratio between the time length of each phase, here indicated by τ_{a} and τ_{r}, respectively, is typically a function of the cadence. When the stroke pace is low, usually the recovery phase is longer, whereas the duration of the two phases gets roughly even for higher values of the cadence.

To estimate the time length of the active and recovery phase we made use of the formulas [2, 7]

$$\tau_{\mathrm{a}}=0.00015625(r-24)^2-0.008125(r-24)+0.8$$

$$\tau_{\mathrm{r}}=\frac{60-\tau_{\mathrm{a}}r}{r}=T-\tau_{\mathrm{a}}$$

These expressions give results in good agreement with the measurements obtained by Brearley and de Mestre from video recordings of actual rowers, which are reported in [6].

DOI: 10.1002/fld

5.1. Oarlocks forces

Oarlock forces are relatively easy to measure, and experimental data are available in the literature, we choose to model the oarlock force by means of the following formula, well fitting measurements:

$$\begin{aligned} f_x^{o^i} &= F_x^{\max} \sin\left(\frac{\pi t}{\tau_a}\right) \\ f_z^{o^i} &= F_z^{\max} \sin\left(\frac{\pi t}{\tau_a}\right) \end{aligned} \tag{15}$$

where typical values of maximum forces are $F_x^{\max} = 1200$ [N] and $F_z^{\max} = 200$ [N]. These values can be changed to suit different athlete characteristics.

5.2. Rowers motion

The motion of each body part of a rower has been reconstructed starting from experimental data obtained by motion capture techniques (see Figure 8) by the team of C. Sforza at the Department of Human Morphology of University of Milan, Italy. In this kind of experiments, light-reflecting markers are applied on an athlete's body, in correspondence to the main articulations. The athlete is then filmed by a set of cameras while rowing on an ergometer, so that the position of the markers at any time instant can be reconstructed by triangulation from the images each camera has recorded. More details on the recording technique may be found in [11], where it has been applied to the analysis of a particular movement of gymnastics.

Starting from these data, the motion time history and the trajectory of each marker has been analyzed, and finally reconstructed by means of analytic functions, which can be parametrized according to the athletes characteristics. As an example, we report in Figure 9 the reconstruction performed for the wrist marker where the path has been approximated by an ellipse. We can note that there is a good repeatability of the gesture, which justify the hypothesis of a periodic motion. Through the use of a standard model of human anatomy it was possible to reconstruct from the marker trajectory the law of motion of the center of mass of each of the body parts we use in our model, i.e. the $\mathbf{x}_{ij}$, $\dot{\mathbf{x}}_{ij}$ and $\ddot{\mathbf{x}}_{ij}$ needed in Equation (14).

Figure 8. Three-dimensional motion analysis during ergometer rowing: body landmarks are marked with retroreflective markers. In the background, two of the TV cameras can be seen.

DOI: 10.1002/fld

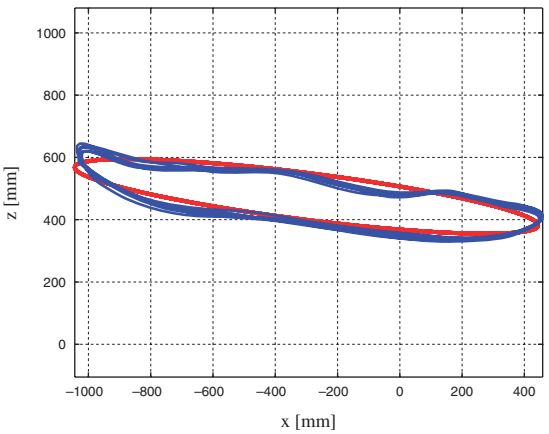

Figure 9. Experimental (darker line-blue in the color version) and reconstructed (lighter ellipse-red in the color version) path in the xz plane of a rower wrist.

6. THE FLUID–STRUCTURE INTERACTION FORCES

Here we deal with forces acting on the hull because of its interaction with the water. We assume we can decompose the forces into terms related to the main motion and those coming from secondary motion.

Forces and momenta induced by the water on the hull during its motion may be decomposed into

$$\begin{aligned} \mathbf{F}^{\mathrm{w}} &= \mathbf{S} - R\mathbf{e}_X + \mathbf{F}^{\mathrm{d}} \\ \mathbf{M}^{\mathrm{w}} &= (M_{\mathrm{S}} + M^{\mathrm{d}})\mathbf{e}_Y \end{aligned} \tag{16}$$

where $\mathbf{S}$ is the lift, R the resistance (the negative sign has been set to have $R \geqslant 0$) and are linked to the main motion, while $\mathbf{F}^{\mathrm{d}}$ is due to the secondary movements. M_{S} and M^{d} are the corresponding angular moments (the resistance forces are assumed to have a negligible couple).

6.1. *The action of the mean motion*

To determine the resistance R, we should in principle solve the equations of fluid dynamics around the hull. Here, we choose instead *to model* it through empirical formulas. The main terms which make up R are the aerodynamic drag and the hydrodynamic resistance, the latter subdivided into *shape*, *wave* and *viscous* resistance, i.e.

$$R = R_{\mathrm{air}} + R_{\mathrm{shape}} + R_{\mathrm{vis}} + R_{\mathrm{wave}} \tag{17}$$

In this work we have considered to neglect R_{air} since its contribution is much smaller than the others. Anyway it can be taken into account using for instance the expression reported in [12]. We will indicate with $|\Gamma^{\mathrm{b}}| = |\Gamma^{\mathrm{b}}(t)|$ the measure of the wetted portion of the hull external surface Γ and with $|\Gamma^{\mathrm{b}}_X|$, $|\Gamma^{\mathrm{b}}_Z|$ its projection on the plane orthogonal to the corresponding axis. The computation of the wetted surface, which changes in time because of the boat movements, will be detailed later on.

DOI: 10.1002/fld

The shape resistance is given by

$$R_{\text{shape}} = \tfrac{1}{2}\rho|\Gamma^{\text{b}}_X|C_{dX}V_X^2$$

where ρ is the water density, V_X the forward boat speed, C_{dX} the shape resistance coefficient. A typical value of C_{dX} is 0.01.

The viscous term comes from two combined effects: skin friction and viscous pressure resistances. For thin ships at low speeds the formula

$$R_{\text{vis}} = \tfrac{1}{2}\rho C_v|\Gamma^{\text{b}}|V_X^2$$

is appropriate, where the drag coefficient C_v approximately equals the skin friction coefficient C_{f}. The latter can be estimated using the ITTC 1957 ship correlation line [13], i.e. the formula

$$C_{\text{f}} = \frac{C_{\text{f0}}}{(\log(Re)-2)^2}$$

Here, $Re = \bar{V}_X L_{\text{M}}/\nu$ is the Reynolds number and L_{M} the mean wetted length (which in our case may be taken equal to the length of the boat), while ν is the kinematic viscosity of water, and finally C_{f0} the asymptotic value for $Re = 0$, usually taken equal to 0.075. As a result, viscous resistance reads

$$R_{\text{vis}} = \tfrac{1}{2}\rho C_{\text{f}}\Gamma^{\text{b}}V_X^2$$

Finally, wave resistance is computed starting from the classical Michell's integral (see [14–16]) to obtain the coefficient C_{dw} in

$$R_{\text{wave}} = \tfrac{1}{2}\rho|\Gamma^{\text{b}}_Z|C_{dw}V_X^2$$

where a suitable value for the range of Froude numbers typical of sculls is $C_{dw} = 0.02$. The accuracy of such equation has been confirmed by the works of [17] (see also [18]). The values of the various coefficients have either been taken from the cited literature or computed by fitting a series of 'off-line' RANSE computation on the boat moving at different configurations.

The terms $\mathbf{S}$ and M_{S} are mainly linked to the action of water pressure on the wetted surface of the hull, whose value is linked to the hydrostatic action and hydrodynamic effects. The latter are important when the vertical component of the velocity are relevant with respect to the other components. For a scull we may consider, as a first approximation, that the dynamic effects on the pressure are not important and the water pressure level around the boat is linked to hydrostatics. Furthermore, we will make the further approximation that we can use the undisturbed water level to compute the hydrostatic pressure.

We then have that the action due to the pressure results in a force

$$\mathbf{S}(t) = -\rho g\int_{\Gamma^{\text{b}}(t)}(h_0 - Z)\mathbf{N}\,\mathrm{d}\gamma$$

where $\mathbf{N}$ is the unit vector normal to the surface $\Gamma^{\text{b}}(t)$, expressed in the absolute reference frame.

The wetted surface changes with time. Let Γ_0 be the external surface of the hull in the hull reference frame. The current configuration $\Gamma^{\text{b}}(t)$ is obtained from Γ_0 by a rigid motion. We can then define the function

$$Q(\mathbf{X}) = \max(0, h_0 - Z)$$

DOI: 10.1002/fld

as well as the corresponding function in the hull reference frame

$$q(\mathbf{x}; G_Z^{\mathrm{h}}, \phi) = \max(0, h_0 + x\sin\phi - z\cos\phi - G_Z^{\mathrm{h}})$$

Consequently we can write

$$\mathbf{S}(t) = -\rho g \int_{\Gamma_0} q(\mathbf{x}, G_Z^{\mathrm{h}}(t), \phi(t)) \mathscr{R}^{\mathrm{T}}(\phi(t)) \mathbf{n}\, \mathrm{d}\gamma$$

The latter surface integral is readily estimated by triangulating the exterior surface of the hull and employing a trapezoidal quadrature rule, leading to the following approximation:

$$\mathbf{S}(t) \simeq -\frac{\rho g}{3} \sum_{k=1}^{n_{\mathrm{t}}} A_k \mathscr{R}^{\mathrm{T}}(\phi(t)) \mathbf{n}_k \left[\sum_{i=1}^{3} q(\mathbf{x}_{k,i}, G_Z^{\mathrm{h}}(t), \phi(t)) \right]$$

Here, n_{t} is the total number of triangles that describe surface Γ_0, A_k and n_k the area and normal of the kth triangle, while $\mathbf{x}_{k,i}$ is the coordinate of its ith vertex.

In the same manner we compute the other surface measures needed in the equations, which define resistance terms. We have

$$|\Gamma^{\mathrm{b}}(t)| = \int_{\Gamma_0} q(\mathbf{x}, G_Z^{\mathrm{h}}(t), \phi(t))\, \mathrm{d}\gamma, \quad |\Gamma_X^{\mathrm{b}}|(t) = \frac{1}{2} \int_{\Gamma_0} q(\mathbf{x}, G_Z^{\mathrm{h}}(t), \phi(t)) |\cos\phi(t) n_x + \sin\phi(t) n_z|\, \mathrm{d}\gamma$$

$$|\Gamma_Z^{\mathrm{b}}|(t) = \left| \int_{\Gamma_0} q(\mathbf{x}, G_Z^{\mathrm{h}}(t), \phi(t))(-\sin\phi(t) n_x + \cos\phi(t) n_z)\, \mathrm{d}\gamma \right|$$

Then the expression of the hydrostatic moment reads

$$M_{\mathrm{S}}(t) = -\rho g \int_{\Gamma_0} q(\mathbf{x}, G_Z^{\mathrm{h}}(t), \phi(t)) \mathbf{x} \times \mathbf{n}\, \mathrm{d}\gamma$$

Before analyzing the effects of the secondary movements that will make possible the computation of $\mathbf{F}^{\mathrm{d}}$ and M^{d}, let us illustrate the structure of the equations when the effect of secondary motions is neglected.

If we define

$$\mathbf{y} = [\dot{G}_X^{\mathrm{h}}, \dot{G}_Z^{\mathrm{h}}, \dot{\phi}, G_X^{\mathrm{h}}, G_Z^{\mathrm{h}}, \phi]^{\mathrm{T}}$$

system (14) can be rearranged in the standard form

$$A(t, \mathbf{y}(t)) \frac{\mathrm{d}\mathbf{y}}{\mathrm{d}t}(t) = \mathbf{B}(t, \mathbf{y}(t)), \quad t > 0 \tag{18}$$

and complemented with initial conditions $\mathbf{y}(0) = \mathbf{y}_0$ ($\mathbf{y}_0$ is usually zero). The first three rows of the 6×6 matrix A and the vector B contain terms arising from Equation (14). The remaining three rows have been generated by the transformation of the second–order differential equations into a first-order system. This form is ready to be integrated by software packages for system of ordinary differential equations.

DOI: 10.1002/fld

6.2. The computation of the effect of secondary motions

In the following sections we will describe the methodology employed to account for the effects of the secondary motions. In particular, we will detail how they generate hydrodynamic forces that superimpose those linked to the mean motion. First, we will show that, thanks to a few simplifying assumptions, the flow field past a boat oscillating in water can be evaluated by solving a linearized potential problem (radiation problem). This procedure is rather common in several applications in naval engineering, see for instance [19, 20], yet, to the best of our knowledge, it is the first time that it is applied to rowing boat dynamics.

Exploiting the linearity of the Laplace equation, such radiation problem can be conveniently decomposed into a series of simpler problems in which we compute the potential corresponding to a single forced harmonic oscillation of the boat, on each of its generalized mode. Finally, we will illustrate how the hydrodynamics forces produced by these potential problems can be effectively modeled by a damping and an added mass term to be added to Equation (18).

We will denote with L_s the length of the scull, and with λ and A the length and the amplitude of the waves related to secondary motions, respectively. We will assume that $\lambda \simeq L_\mathrm{s}$ and $A \ll L_\mathrm{s}$, which imply that the waves generated by the secondary movements are rather long but of small amplitude compared with the dimension of the boat, in line with what is generally observed. We also suppose that the boat motion is periodic, having period T and an angular frequency $\omega = 2\pi/T$. Furthermore, we assume that the water flow induced by the secondary motions is irrotational i.e. there exist a potential ψ such that the water velocity $\mathbf{u}$ is equal to $\nabla\psi$, where $\psi = \psi(t, X, Y, Z)$. Since $\mathbf{u}$ is solenoidal we have $\Delta\psi = 0$ on Ω and at all times. In this approximation we considered a fixed geometry and the boundary condition for the potential problem impose that the normal derivative of ψ must match the normal component of the velocity of the boat surface, while the solution must decay at the far field.

To understand how the interaction with the water affects our dynamical system we need to decompose the secondary motion into their different components and assume a periodic motion. To this purpose, we introduce the following notation. We denote with $\mathbf{v} = [v_1, v_2, v_3]^\mathrm{T} = [\dot{G}^\mathrm{s}_X, \dot{G}^\mathrm{s}_Z, \dot{\phi}^\mathrm{s}]^\mathrm{T}$ the vector containing the secondary motion velocities of the boat, which here act as forcing term, and with $\mathcal{N} = [\mathcal{N}_1, \mathcal{N}_2, \mathcal{N}_3]^\mathrm{T} = [n_x, n_z, -xn_z + zn_x]^\mathrm{T}$ the so-called *generalized normal vector* [19], which permits to adopt the same expression for the linear and angular movements.

The periodic motion is characterized by a fundamental period T and the corresponding angular frequency $\omega = 2\pi/T$.

6.3. The computation of the potential flow

The periodic motion resulting from the sum of harmonic components characterized by an angular frequency, which is a multiple of the fundamental angular frequency. Thanks to the linearity of the problem we can just consider a generic component with angular frequency ω. Thus, the velocities can be expressed in the form

$$v_s(t) = \mathrm{Re}(\Upsilon_s \, \mathrm{e}^{-\mathrm{i}\omega t}), \quad s = 1, 2, 3$$

where i indicates the imaginary unit and the Υ_s are complex values accounting for the amplitude and phase shift of the s component of the secondary motion (we will see, however, that eventually they do not play any role). As usual, $\mathrm{Re}(z)$ and $\mathrm{Im}(z)$ denote the real and imaginary part of the complex number z, respectively.

DOI: 10.1002/fld

Correspondingly, the fluid potential takes the form

$$\psi(t,\mathbf{X})=\mathrm{Re}(\Psi(\mathbf{X})\mathrm{e}^{-\mathrm{i}\omega t}),\quad s=1,2,3 \tag{19}$$

where Ψ is a complex valued function that can be written as the sum of three contributions proportional to the corresponding velocity component of the secondary motion, i.e.

$$\Psi(\mathbf{X})=\sum_{s=1}^{3}\Upsilon_s\Psi_s(\mathbf{X})$$

Let us consider Figure 10 where $\Omega=\{\mathbf{X}\in\mathbb{R}^2\times[h_0,h_0-H]\}\setminus\Omega_\mathrm{b}$, here Ω_b indicating the scull and H being the total depth of the channel (which is assumed constant).

The boundary of Ω comprises three parts: the wet surface of the scull Γ_0^b, the bottom Γ_f and the free surface Γ_w. In the following we will consider also the domain $\widehat{\Omega}$, which is the intersection between Ω and a vertical cylinder with radius $R\gg L$ and vertical axis passing through the barycenter of the scull; Σ is the portion of $\partial\widehat{\Omega}$ corresponding to the lateral surface of the cylinder whereas $r=\sqrt{X^2+Y^2}$ will denote the radial coordinate.

The complex potential Ψ_s satisfies the following differential problem:

$$-\Delta\Psi_s=0\quad\text{in }\Omega \tag{20a}$$

$$\frac{\partial\Psi_s}{\partial Z}=0\quad\text{on }\Gamma^\mathrm{f} \tag{20b}$$

$$\frac{\partial\Psi_s}{\partial Z}-\frac{\omega^2}{g}\Psi_s=0\quad\text{on }\Gamma^\mathrm{w} \tag{20c}$$

$$\frac{\partial\Psi_s}{\partial n}=\mathcal{N}_s\quad\text{on }\Gamma_0^\mathrm{b} \tag{20d}$$

$$R^{1/2}\left(\frac{\partial\Psi_s}{\partial r}-\mathrm{i}\kappa\Psi_s\right)\to 0\quad\text{for } R\to\infty \tag{20e}$$

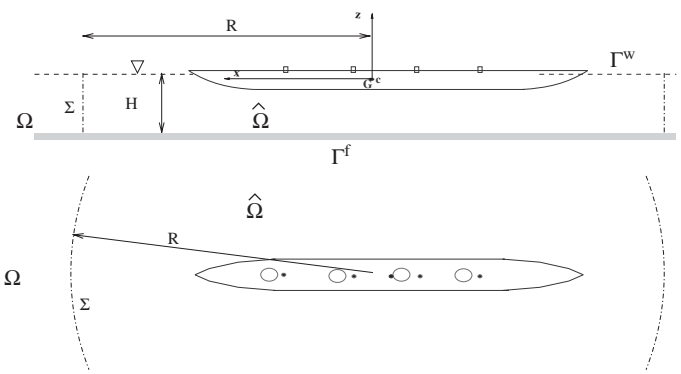

Figure 10. Domain for the full potential computation.

DOI: 10.1002/fld

We recall that the scull has been considered in the reference position and we have neglected the changes in Γ^{f} induced by the water waves. Again, this approximation is justified by the hypothesis of waves of small amplitude and is anyway necessary to linearize the problem.

Equation (20d) relates Ψ_s with the geometry of the scull. Condition (20e) is the decay condition at infinity where κ is the wave number which the only real root of the dispersion relation

$$k\tanh(kH)=\frac{\omega^2}{g}$$

Assuming that $\kappa H=2\pi H/\lambda\gg 1$ (i.e. waves that are short with respect to the depth of the basin) we have $\kappa=\omega^2/g$.

Formulation (20) is not suitable for numerical implementation; a possible alternative is to consider the problem in $\widehat{\Omega}$: in this case the decay relation has to be transformed into a *suitable radiation condition* on Σ. Problem (20) is then replaced by

$$-\Delta\Psi_s=0 \quad \text{in } \widehat{\Omega} \tag{21a}$$

$$\frac{\partial\Psi_s}{\partial Z}=0 \quad \text{on } \widehat{\Gamma}^{\mathrm{f}} \tag{21b}$$

$$\frac{\partial\Psi_s}{\partial Z}-\frac{\omega^2}{g}\Psi_s=0 \quad \text{on } \widehat{\Gamma}^{w} \tag{21c}$$

$$\frac{\partial\Psi_s}{\partial n}=\mathscr{N}_s \quad \text{on } \Gamma_0^{\mathrm{b}} \tag{21d}$$

$$\frac{\partial\Psi_s}{\partial n}=-\mathscr{C}(\Psi_s) \quad \text{on } \Sigma \tag{21e}$$

Here $\mathscr{C}$ is the operator that associates to the trace of Ψ_s on Σ the normal derivative $\partial\Psi_s/\partial n$ such that the solution of (21) is the restriction in $\widehat{\Omega}$ of the solution of (20). It can be approximated by using *localized* or *hybrid* finite elements [21, 22] or *localized boundary element* [23, 24]. A simpler technique is to use a *first-order* radiation condition, by which

$$\mathscr{C}(\Psi_s)=-\mathrm{i}\kappa\Psi_s$$

and this is the condition we have used in our numerical experiments.

6.4. Added mass and damping matrix

Given our assumptions on the wavelengths and wave amplitudes, the dynamic pressure p_{d} induced by secondary motions can be approximated by using the *generalized Bernoulli equation*, thus neglecting the *nonlinear terms* [19]. Hence, we have

$$p_{\mathrm{d}}=-\rho\frac{\partial\psi}{\partial t}$$

The force and momentum generated by the dynamic pressure on the hull will be contained in the *restoring force vector* $\mathscr{F}^{\mathrm{d}}=[F_X^{\mathrm{d}},F_Z^{\mathrm{d}},M^{\mathrm{d}}]^{\mathrm{T}}$, which can be computed by

$$\mathscr{F}^{\mathrm{d}}=-\rho\int_{\Gamma_0^{\mathrm{b}}}\frac{\partial\psi}{\partial t}\mathscr{N}\,\mathrm{d}\gamma \tag{22}$$

DOI: 10.1002/fld

Once computed, the potentials Ψ_s $(s=1,2,3)$ can be plugged in Equations (19) and (22) to obtain $\mathscr{F}^{\mathrm{d}}$. To this aim, we define the *restoring force matrix*

$$f_{st}=\mathrm{i}\rho\omega\int_{\Gamma_0^{\mathrm{b}}}\Psi_s\mathscr{N}_t\,\mathrm{d}\gamma,\quad s,t=1,2,3 \tag{23}$$

each component representing the hydrodynamic reaction in the direction t due to the component s of the movement of the boat. Employing the standard convention for the summation of repeated indexes, we can now compute the tth component of $\mathscr{F}^{\mathrm{d}}$ as

$$\begin{aligned}\mathscr{F}_t^{\mathrm{d}}&=\mathrm{Re}(\Upsilon_s f_{st}\mathrm{e}^{-\mathrm{i}\omega t})=\mathrm{Re}[(\mathrm{Re}\,f_{st}+\mathrm{i}\,\mathrm{Im}\,f_{st})\Upsilon_s\,\mathrm{e}^{-\mathrm{i}\omega t}]\\&=\mathrm{Re}\left[\left(\mathrm{i}\rho\omega\int_{\Gamma_0^{\mathrm{b}}}\mathrm{Re}\,\Psi_s\mathscr{N}_t\,\mathrm{d}\gamma-\rho\omega\int_{\Gamma_0^{\mathrm{b}}}\mathrm{Im}\,\Psi_s\mathscr{N}_t\,\mathrm{d}\gamma\right)\Upsilon_s\mathrm{e}^{-\mathrm{i}\omega t}\right]\\&=-\left(\rho\int_{\Gamma_0^{\mathrm{b}}}\mathrm{Re}\,\Psi_s\mathscr{N}_t\,\mathrm{d}\gamma\right)\dot{v}_s(t)-\left(\rho\omega\int_{\Gamma_0^{\mathrm{b}}}\mathrm{Im}\,\Psi_s\mathscr{N}_t\,\mathrm{d}\gamma\right)v_s(t)\end{aligned}$$

This formula puts into evidence that the restoring force vector can be split into two terms, one proportional to the boat secondary acceleration $\dot{v}_s$, and the other proportional to the secondary velocity v_s. Physically speaking, the forces due to the secondary motions have a double effect on the dynamics of the scull. The term proportional to accelerations induces an *added mass* term, which effectively increases the boat mass in the dynamical system. The term proportional to the velocity is instead a damping term, and it accounts for dissipative effects associated to the radiation at infinity of the water waves generated by the motion.

As for the modification to our dynamical system, they are better identified by defining the added mass and the damping matrices [19], here indicated by $\mathscr{M}$ and $\mathscr{S}$, respectively. They are given by

$$\mathscr{M}_{st}=\rho\int_{\Gamma_0^{\mathrm{b}}}\mathrm{Re}(\Psi_s)\mathscr{N}_t\,\mathrm{d}\gamma\quad\text{and}\quad\mathscr{S}_{st}=\rho\omega\int_{\Gamma_0^{\mathrm{b}}}\mathrm{Im}(\Psi_s)\mathscr{N}_t\,\mathrm{d}\gamma,\quad s,t=1,2,3$$

These matrices are symmetric and positive definite, and only depend on the boat geometry. For this reason, they can be conveniently computed 'off-line'.

To modify dynamical system (18) we extend by zero the damping and added mass matrices to produce two 6×6 matrices $\widehat{\mathscr{M}}$ and $\widehat{\mathscr{S}}$, as follows:

$$\widehat{\mathscr{M}}=\begin{bmatrix}\mathscr{M}&\mathbf{0}\\\mathbf{0}&\mathbf{0}\end{bmatrix}\quad\text{and}\quad\widehat{\mathscr{S}}=\begin{bmatrix}\mathscr{S}&\mathbf{0}\\\mathbf{0}&\mathbf{0}\end{bmatrix}$$

and the dynamical system now becomes

$$\widehat{\mathbf{A}}(\mathbf{y}(t),t)\frac{\mathrm{d}\mathbf{y}}{\mathrm{d}t}(t)=\widehat{\mathbf{B}}(\mathbf{y}(t),t),\quad t>0$$

where $\widehat{A}(\mathbf{y}(t),t)=A(\mathbf{y}(t),t)+\widehat{\mathscr{M}}$ and $\widehat{\mathbf{B}}(\mathbf{y},t)=\mathbf{B}(\mathbf{y},t)-\widehat{\mathscr{S}}\mathbf{y}$.

DOI: 10.1002/fld

This system of ordinary differential equation, has to be supplemented by initial condition, which usually correspond to a zero velocity of the boat at $t=0$. It has been solved using the explicit Runge–Kutta adaptive scheme available in the Gnu Scientific Library [25]. The energy E_d dissipated by the secondary motions during one period can be computed as $E_\mathrm{d}=\frac{1}{2}\int_{t_0}^{t_0+T}\mathbf{y}^\mathrm{T}(t)\widehat{\mathscr{S}}\mathbf{y}(t)\,\mathrm{d}t$. It has been found to be as much as approximately 10% of the total energy dissipation, justifying to account for the effect of secondary motions in the dynamical model.

What done so far considers a single harmonic mode only. The actual motion is a superimposition of harmonics. This fact can be accounted for by using convolution techniques. Yet, it has been found that the fundamental mode is the one responsible for great part of the energy dissipation. Therefore, for the sake of simplicity, we have considered in this work only the fundamental mode, whose period is equal to that of the rowing cadence.

7. NUMERICAL SOLUTION AND EXAMPLES

To compute the added mass and damping matrices, we only need to know the values of the potential field on the boat surface. Hence, problem (21) has been solved by means of a boundary element method based on the free-space Green's function. The boundary of the domain $\widehat{\Omega}$ has been discretized by means of a set of curved quadrilateral elements defined by eight nodes each (see [26]). Contours of the elevation of the free surface, namely

$$\eta(x,y)=\mathrm{Re}\left\{\frac{\mathrm{i}\omega}{g}\Psi_s(x,y,0)\right\} \tag{24}$$

for the hull of a four rowers boat oscillating at a frequency $\omega=4.136\,\mathrm{rad/s}$ in the heave ($s=2$) and pitch ($s=3$) direction are presented in Figure 11.

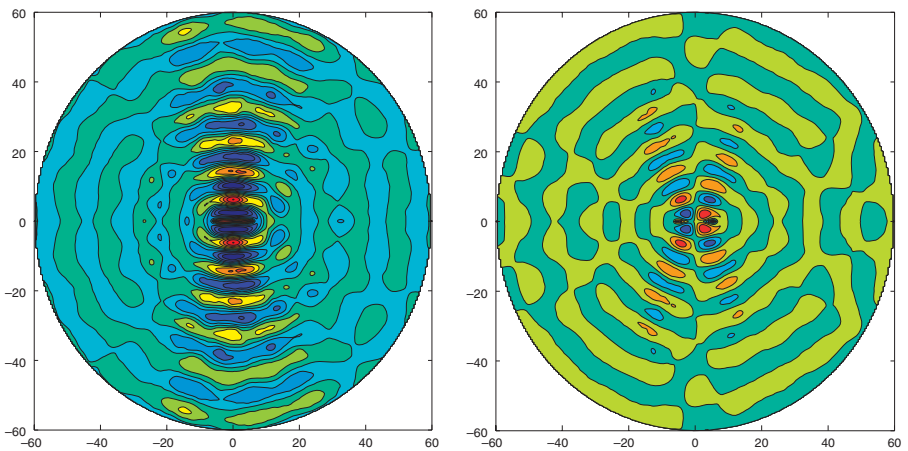

Figure 11. Predicted wave patterns when the boat is oscillating in the heave (left) and pitch (right) direction.

DOI: 10.1002/fld

The resulting damping and added mass matrices are

$$\mathscr{S} = \begin{bmatrix} 0.593 & 2.728 & 68.202 \\ 2.728 & 1028.523 & 188.381 \\ 68.202 & 188.381 & 7934.294 \end{bmatrix}, \quad \mathscr{M} = \begin{bmatrix} 0.201 & 0.445 & 17.221 \\ 0.445 & 226.102 & 21.905 \\ 17.221 & 21.905 & 1478.847 \end{bmatrix}$$

The mathematical model described in the previous sections has been implemented in a software code, which takes as input all the data concerning the boat geometry and type, rowers motion and weights, the coefficient for the various forcing terms.

It has been used first to reproduce available measurements data. In Figure 12, on the left, we report the horizontal velocity time history measured on a single scull driven at 20 strokes per minute by a female rower. No data on the rower were available for these measurements, and both the physical characteristics and maximum oarlock force had to be reconstructed. We supposed therefore that the rower weight is 60 kg, her height is 1.70 m, while we assumed $F_x^{\max} = 1000\,\mathrm{N}$ and $F_z^{\max} = 150\,\mathrm{N}$ for the oarlock values.

Moreover, the geometrical configuration of the boat was unknown, and feasible values have been adopted. The hull employed for the simulation is 8.2 m long, the footboard horizontal and vertical distances from the stern are 3.4 and -0.05 m, respectively, while the oarlocks are placed 3.8 m ahead of the stern, and 0.2 m over it. The boat hull weight is 15 kg and the moment of inertia around the pitching axis is $66\,\mathrm{kg\,m^2}$.

The computed time history for the horizontal velocity (Figure 12, right) shows an excellent qualitative agreement with the experiments, although differences between measured and computed values can be observed in correspondence with the beginning of each stroke.

Considering the uncertainties on the experimental set up, it would be very difficult to assess if the differences are due to the approximations in the numerical model. More experimental data are being collected and will be used to tailor the model further.

Besides computing the horizontal velocity, our software predicts the full dynamics of a rowing boat in its symmetry plane, once the boat geometrical data, and proper physical characteristics and kinematics of the rowers are provided.

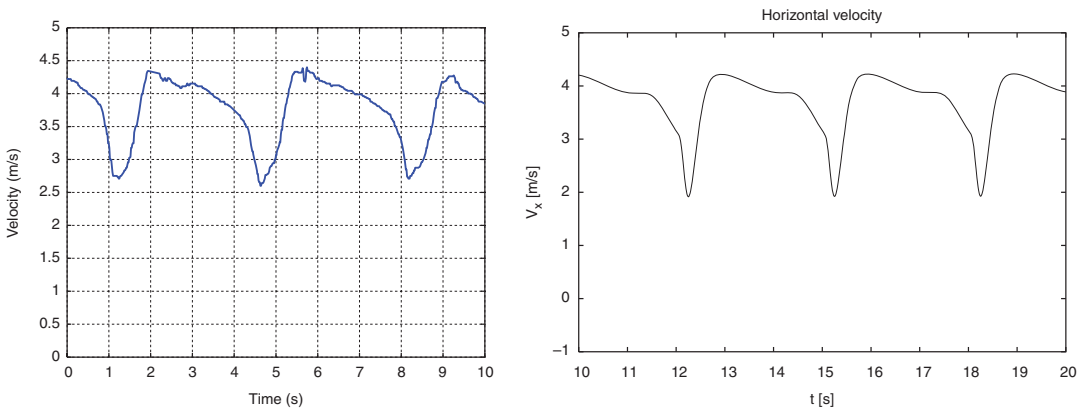

Figure 12. Measured (left) and computed (right) time history of velocity for a single scull.

DOI: 10.1002/fld

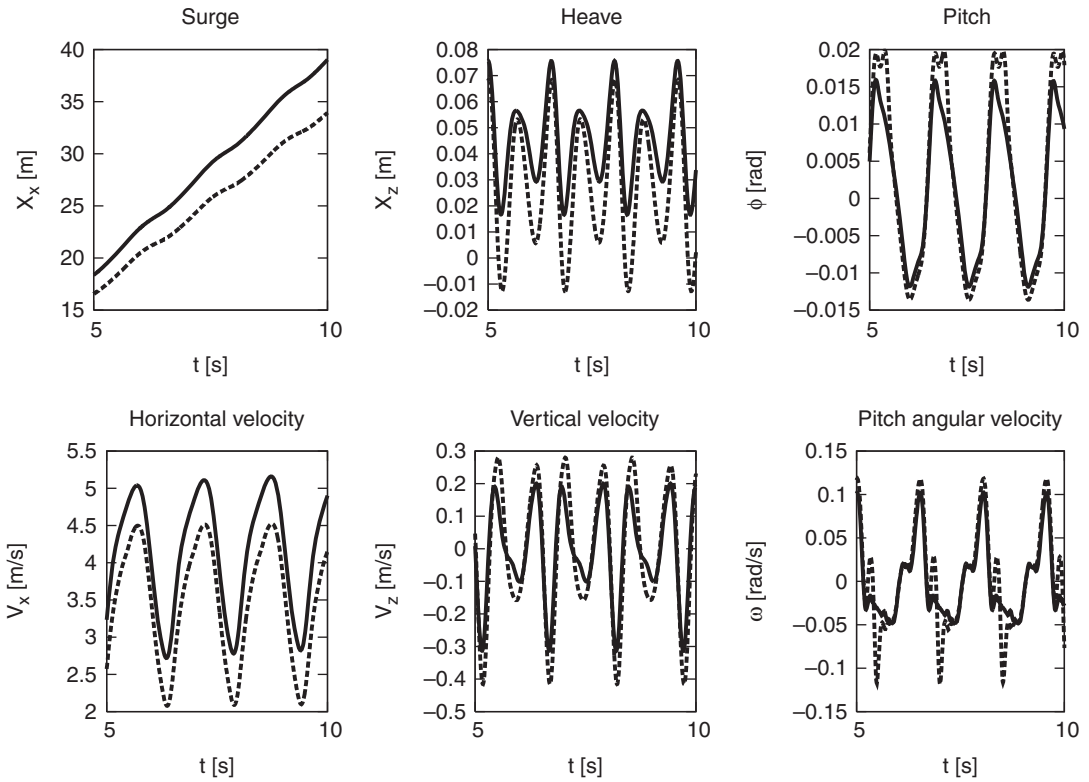

Figure 13. Positions and velocities for a single scull pushed by two different rowers. The first weighting 106 kg (dashed line) and the second 80 kg (continuous line).

A characteristic output for a single scull is depicted in Figure 13, showing the time histories for positions and velocities along X and Z directions, as well as pitch angle and angular velocity time histories for two different singles sculls. Here we compare the performance of two rowers having different weights, pushing with the same force (1200 N) and at the same pace (39.5 strokes per minute), on the same boat.

As expected, the boat with the heavier rower proceeds with a deeper sinkage, which causes a larger wet surface and hence higher drag. Furthermore, the secondary movements, in particular heaving, are more marked for the heavier rower. The obvious consequence is a reduction of the speed with respect to the boat with lighter rower. To obtain the same performance the heavier rower has to push harder and possibly change rowing style. Being able to assess rapidly the performance changes due to a modification of the rower characteristics makes this model potentially useful also for trainers and athletes.

Finally, we present an example of how the program can be employed in the design process of rowing boats. Figure 14 shows the comparison among the predicted performances of three different 4*x* sculls. To study the optimal longitudinal positioning of the athletes along the boat, we compared three different longitudinal positions of the crew on the boat. Starting from a reference position, in one case the rowers are displaced of 10 cm toward the boat bow, whereas in the other they are

DOI: 10.1002/fld

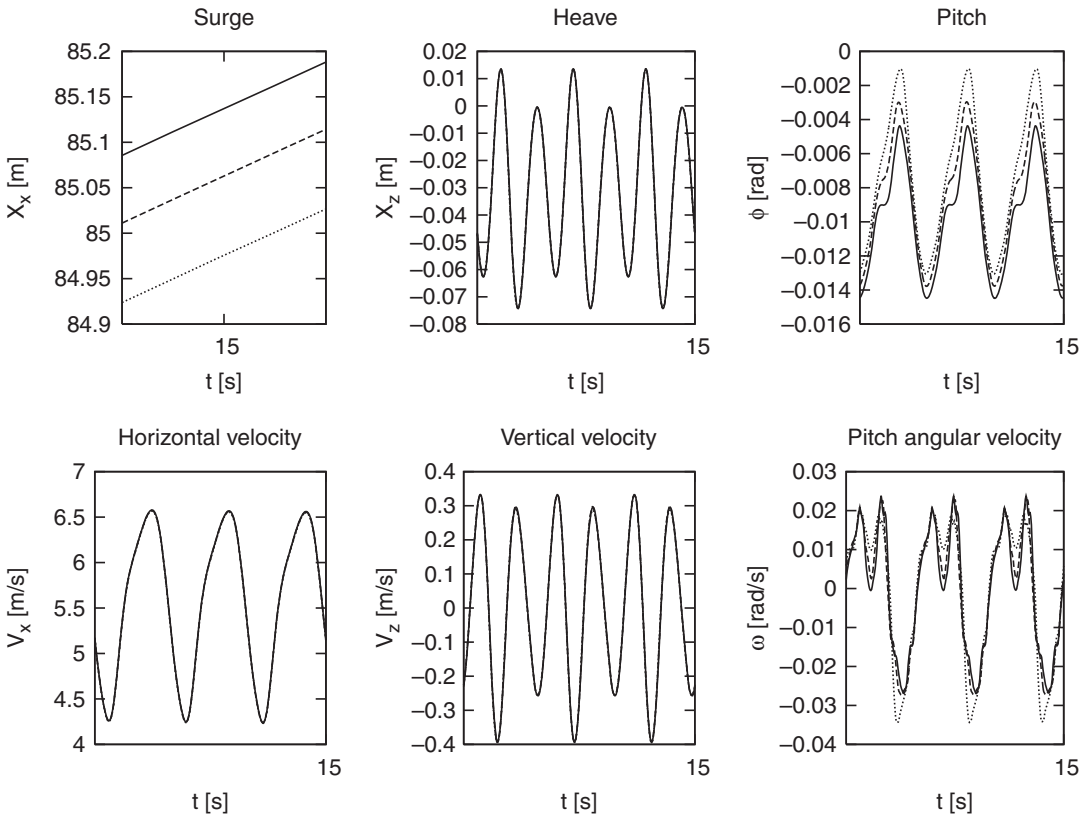

Figure 14. Positions and velocities for a four scull pushed by rowers placed in three different longitudinal positions on the boat. Athletes are moved aft (continuous line) and forward (dotted line) with respect to a reference position (dashed line).

moved 10 cm toward the stern. The result show potential beneficial effects of rowers displacement in the aft direction. The impact of these differences on the race can be evaluated by considering that for a 2000 m race field the aft position presents an advantage on the other configurations of 2 and 4 m, respectively. It may look a small quantity, however, races are often won by tiny differences.

8. CONCLUSIONS

We have developed a rather complete model for sculls, which comprises both the fluid–structure interaction, and the mechanical system composed of athletes, shell and oars. The model takes into account the athlete and boat characteristics and can be employed for boat design, performance prediction as well as support to training.

The objective was to have an accurate yet computationally efficient tool, hence the choice of a reduced hydrodynamic modeling. However, the dynamical model can be readily coupled with

DOI: 10.1002/fld

codes based on the full Navier–Stokes equation with free surface modeling. Indeed, this is also part of our current activity and some preliminary results have been published in [27, 28]. Clearly, the computational cost of this latter approach is much higher (several hours compared with minutes). Therefore, its use may be justified only at the final stages of the design cycle, while the model presented in this work is of great help in the early stages, as it allows to test different configurations very rapidly. Another possible use of the model is the analysis of different crew arrangements and dynamics by coaches and trainers.

We have here considered the motion in the symmetry plane, assuming a scull type of rowing boat and experienced rowers. However, a more complete three-dimensional model is under investigation, to study boat stability, and sweep boats dynamics.

ACKNOWLEDGEMENTS

The authors would like to thank Filippi Lido S.r.L for financial and technical support, and in particular Alessandro Placido. Thanks to the team of Chiarella Sforza at University of Milan for the availability of the image capturing data. We also acknowledge the help of Luca Del Grosso for the early development of the dynamical model.

REFERENCES

1. Alexander FH. The theory of rowing. In *Proceedings of the University of Durham Philosophical Society*, Todd GW (ed.), vol. VI. Andrew Reid & Co.: Newcastle-upon-Tyne, England, 1925.
2. Atkinson WC. Modeling the dynamics of rowing. Available from: www.atkinsopht.com/row/rowabstr.htm, 2002.
3. Dudhia A. The physics of rowing. Available from: www.atm.ox.ac.uk/rowing/physics, 2001.
4. van Holst M. On rowing. Available from: http://home.hccnet.nl/m.holst/RoeiWeb.html, 2004.
5. Lazauskas L. A performance prediction model for rowing races. *Technical Report L9702*, Department of Applied Mathematics, University of Adelaide, Australia, 1997.
6. Elliott B, Lyttle A, Burkett O. The RowPerfect ergometer: a training aid for on-water single scull rowing. Available from: http://www.rowperfect.com.au, 2004.
7. Rekers CJN. Verification of the RowPerfect ergometer. Available from: www.rowperfect.com/tek19021, Presented at the A.R.A. Senior rowing conference, London, October 1993.
8. Azcueta R. Computation of turbulent free-surface flows around ships and floating bodies. *Ship Technology Research* 2002; **49**(2):46–69.
9. Parolini N, Quarteroni A. Modelling and numerical simulation for yacht design. *Proceedings of the 26th Symposium on Naval Hydrodynamics*, Rome, Italy, 17–22 September 2006.
10. *Man–System Interaction Standards—Volume 1*. NASA Technical Standards, 1995.
11. Grassi GP, Santini T, Lovecchio N, Turci M, Ferrario VF, Sforza C. Spatiotemporal consistency of trajectories in gymnastics: a three-dimensional analysis of flic-flac. *International Journal of Sports Medicine* 2005; **26**(2): 134–138.
12. Millward A. A study of the forces exerted by an oarsman and the effect on boat speed. *Journal of Sports Sciences* 1987; **5**:93–103.
13. Hadler JB. Coefficients for international towing tank conference 1957 model-ship correlation line. *Technical Report 1185*, David Taylor Model Basin, April 1958.
14. Michell JH. The wave resistance of a ship. *Philosophical Magazine* 1898; **45**:106–123.
15. Tuck EO. Wave resistance of thin ships and catamarans. *Applied Mathematics Report T8701*, The University of Adelaide, January 1987.
16. Tuck EO. The wave resistance formula of J.H. Michell (1898) and its significance to recent research in ship hydrodynamics. *Journal of the Australian Mathematical Society* 1989; **30**:365–377.
17. Hanhirova K, Rintala S, Karppinen T. Preliminary resistance prediction method for fast mono- and multihull vessels. *International Symposium on High Speed Vessels for Transport and Defense*, RINA, London, U.K., 23–24 November 1995.

DOI: 10.1002/fld

18. Tuck EO, Scullen DC, Lazauskas L. Wave patterns and minimum wave resistance for high-speed vessel. *24th Symposium on Naval Hydrodynamics*, Fukuoka, Japan, July 2002.
19. Mei CC. *The Applied Dynamics of Ocean Surface Waves*. World Scientific Publishing: Singapore, 1989. Second printing with corrections.
20. Newman Marine JN. *Hydrodynamics*. MIT Press: Cambridge, MA, 1977.
21. Mei CC, Chen HS. A hybrid element method for steady linearized free-surface flows. *International Journal for Numerical Methods in Engineering* 1976; **10**:1153–1175.
22. Lenoir M, Tounsi A. The localized finite element method and its application to the two-dimensional sea-keeping problem. *SIAM Journal on Numerical Analysis* 1988; **25**:729–755.
23. Doppel K, Hochmuth R. An application of the limiting absorption principle to a mixed boundary value problem in an infinite strip. *Mathematical Methods in the Applied Sciences* 1995; **18**:529–548.
24. Hochmuth R. A localised boundary element method for the floating body problem. *IMA Journal of Numerical Analysis* 2001; **21**:799–816.
25. Galassi M, Davies J, Theiler J, Gough B, Jungman G, Booth M, Rossi F. *GNU Scientific Library Reference Manual* (2nd edn). Network Theory Ltd., 2004.
26. Brebbia CA. *The Boundary Element Method for Engineers*. Pentech Press: Plymouth, 1980.
27. Formaggia L, Miglio E, Mola A, Parolini N. Fluid–structure interaction problems in free-surface flows: application to boat dynamics. *International Journal for Numerical Methods in Fluids* 2008; **56**(8):965–978.
28. Formaggia L, Miglio E, Mola A, Scotti A. Numerical simulation of the dynamics of boats by a variational inequality approach. *Proceedings of the 47th Workshop of the International School of Mathematics* '*Guido Stampacchia*' *on Variational Analysis and Aerospace Engineering*, Erice, Italy, 8–16 September 2007.

DOI: 10.1002/fld